Taylor & Francis
Taylor & Francis Group

A scaffoldless technique for self-generation of three-dimensional keratinospheroids on liquid crystal surfaces

CF Soon[1,2], KT Thong[1], KS Tee[1], AB Ismail[2], M Denyer[3], MK Ahmad[1], YH Kong[4], P Vyomesh[4], SC Cheong[4]

[1]Faculty of Electrical and Electronic Engineering, [2]Biosensor and Bioengineering Laboratory, MiNT-SRC, Universiti Tun Hussein Onn Malaysia, Parit Raja, Batu Pahat, Johor, Malaysia, [3]School of Medical Sciences, University of Bradford, Bradford, United Kingdom, and [4]Cancer Research Malaysia, Subang Jaya, Selangor, Malaysia

Accepted February 23, 2016

Abstract

We describe a new scaffold-free three-dimensional (3D) cell culture model using cholesteryl ester based lyotropic liquid crystal (LC) substrates. Keratinocytes were deposited randomly on the LC surface where they self-assembled into 3D microtissues or keratinospheroids. The cell density required to form spheroids was optimized. We investigated cell viability using dead/live cell assays. The adhesion characteristics of cells within the microtissues were determined using histological sectioning and immunofluorescence staining. Fourier transform infrared spectroscopy (FTIR) was used to characterize the biochemistry of the keratinospheroids. We found that both cells and microtissues could migrate on the LC surface. The viability study indicated approximately 80% viability of cells in the microtissues up to 20 days of culture. Strong intercellular adhesion was observed in the stratification of the multi-layered microspheroids using field emission-scanning electron microscopy (FE-SEM) and histochemical staining. The cytoskeleton and vinculins of the cells in the microtissues were expressed diffusely, but the microtissues were enriched with lipids and nucleic acids, which indicates close resemblance to the conditions in vivo. The basic 3D culture model based on LC may be used for cell and microtissue migration studies in response to cytochemical treatment.

Key words: aggregates, cell culture, cell viability, cholesteric liquid crystal, cytoskeleton, Fourier transform infrared spectrometry, keratinocytes, keratinospheroids, live/dead cell assay, microtissues, scaffolds, self-assembly, self-generation, spheroids, three-dimensional cell culture

The use of two-dimensional (2D) cell cultures in plastic flasks has limitations for studying cell physiology and the effects of therapeutic drugs (Amann et al. 2014, Ferro et al. 2014, Kunz-Schughart et al. 2004). Monolayers of cells in 2D cultures are flattened and tightly adherent to the culture flasks. With only a portion of the cell surface exposed to the culture medium in 2D cell, biological responses may differ significantly from those obtained using three-dimensional (3D) microtissue models, which are multicellular aggregations that are organized into a spherical or oval shape (Ferro et al. 2014). Macromolecules that are highly expressed in 2D cell cultures may scarcely be detected in 3D cell culture systems (Grabowska et al. 2011, Peyton et al. 2008). Nonetheless, the structure of cultured cells in 3D environments resemble their condition in vivo, and 3D culture preserves their native functionality (Hsieh et al. 2011, Huh et al. 2011).

Correspondence: Chin Fhong Soon, Biosensor and Bioengineering Laboratory, Faculty of Electrical and Electronic Engineering, Universiti Tun Hussein Onn Malaysia, 86400 Parit Raja, Batu Pahat, Johor, Malaysia. Phone: +6(0)74538614, fax: +6(0)74536060, e-mail: soon@uthm.edu.my

Color versions of one or more of the figures in the article can be found online at www.tandfonline.com/ibih

Biotechnic & Histochemistry 2016, **91(4): 283–295.**

DOI: 10.3109/10520295.2016.1158865

Commercial products are available to produce 3D cell cultures including gravityPLUS™, 3D Petri Dish®, and HydroMatrix™. These products stimulate the growth of 3D microtissues or microspheroids based on one of three techniques: pendant drop, micromolds or composite hydrogel. These techniques have been used to study cell differentiation, drug metabolism, protein expressions, proliferation and responses to stimuli (Harma et al. 2010, Loessner et al. 2010, Napolitano et al. 2007). The pendant drop technique allows cells to aggregate under the influence of the beads of liquid that hang from an array of micropores (Ferro et al. 2014). Micromolds (3D Petri Dish®) cast an agarose gel into microbowls that shape the growth of cell aggregates (Svoronos et al. 2014). Composite hydrogel, such as HydroMatrix, are based on a 3D nanofiber scaffold that promotes cell aggregation, but includes undisclosed proprietary soluble factors. The pendant drop and micromold techniques currently are popular for 3D cell culture research (Amann et al. 2014, Lee et al. 2013). The common features of these two techniques are the curved vessel, gravitational force and interfacial tension that together force the cells into close proximity followed by re-establishment of intercellular contacts.

Currently available 3D culture techniques may not be suitable for epithelial cells. Epithelial cells can migrate, self-assemble and self-organize into 3D structure in the in vivo systems by sensing and responding to physical changes of the microenvironment that surrounds them (Ingber 2006). 3D culture techniques that rely on confining cells in a receptacle would not allow observation of the migration of epithelial cells during the formation of 3D microtissues.

We propose the use of a planar liquid crystal (LC) surface as a scaffoldless cell culture substrate for creating 3D microtissues of keratinocytes or keratinospheroids. In our earlier study (Soon et al. 2014a), we demonstrated that human keratinocytes attached and replicated on cholesteryl ester LC-coated cell culture substrates without pre-functionalization with extracellular matrix (ECM) proteins. Cells cultured at low density (10^4 cells/cm^2) attached to the soft LC surface, and well organized vinculin and dispersed actin filaments appeared at the periphery of the cell membrane (Soon et al. 2014a). The soft compliance of the cholesteryl ester LC might have provided suitable stiffness to allow the adhesion of cells (Soon et al. 2011). In addition to biophysical expressions, the cells on LC assumed a round and compact morphology as shown by wide field surface plasmon microscopy (Soon et al. 2013a). This could be explained by the stiffness of the LC, which likely stimulated the morphological changes of the cells (Soon et al. 2011).

Unlike hydrogels, which are characterized by scaffolds of nanofibers, semisolid LC is characterized by highly compact arrangements of amphiphilic molecules. After interaction with the culture medium, the amphiphilic molecules at the surface of the cholesteric LC re-orient into lyotropic lamellar LC (Soon et al. 2011). In the lyotropic lamellar system, the amphiphilic LC molecules self-assemble into bilayers of lipid molecules that are interspersed with layers of water molecules (Soon et al. 2011). These patterns of lyotropic LC can be found in the essential elements of biological systems including lipid membrane bilayers, nucleic acids and proteins (Bruce et al. 2006, Hata et al. 1980, Small 1977). An earlier study using Fourier transform infrared spectroscopy (FTIR) demonstrated that the cholesteryl ester LC consisted of compounds characterized by hydroxyl and cholesteryl ester groups (Soon et al. 2014a). Cholesterol moieties appear to possess a lyotropic system and stiffness that are similar to the bi-layer lipid membrane of cells, which encouraged cells to attach and proliferate (Hwang et al. 2002, Soon et al. 2014a). In addition, cholesteryl ester occupies 20% of the extracellular space of the stratum corneum (Norlen et al. 2007). When cholesterol is required for the cell membrane and lipoprotein formation, cholesterol ester can be hydrolyzed to release cholesterol, which is essential for cell membrane formation and for stabilizing bilayer lipid membranes (Feingold 2007). An earlier report (Kravchenko et al. 2011) demonstrated that cholesterol esters enhance transdermal delivery of biomolecules. Esterification of cholesterol is vital to keratinization of epidermis (Unna and Goldsdetz 1910). Culturing cells on ester based cholesteryl LC also increases the lipid content in the culture, which favors cell adhesion.

We describe here the self-assembly and growth of keratinocytes into keratinospheroids (growth phase) entering the dormant phase on a LC surface. During the dormant phase, cells stop proliferating and maintain a stationary state until they die during the necrosis phase, during which the spheroids shrink (Folkman and Hochberg 1973). We characterized the biophysical properties of the microtissues and investigated the structural organization of cells in the microtissues using field emission scanning electron microscopy (FE-SEM), immunofluorescence staining, live/dead cell viability assay, FTIR, and histological sectioning and staining. We also compared the biophysical properties of the microtissues formed using LC and compared these with cells grown in monolayers.

Material and methods

Preparation of LC substrate

We used cholesteryl ester LC as a substrate for 3D cultures. Mixtures of cholesteryl pelargonate, cholesteryl chloride and cholesteryl oleyl carbonate were melted to isotropic phase at 118° C in a glass vial as described previously (Soon et al. 2014a). The isotropic phase is a liquid state in which the LC molecules have no organized orientation. While in the isotropic phase, the LC was applied to the surface of a petri dish to create a controlled coating approximately 300 μm thick using a squeegee coating machine that we developed (Soon et al. 2014b). The area of the LC coating was approximately 1.5×3 cm^2. During the coating process, the LC gel formed a light greenish cholesteric LC substrate. The spreading created shear stress that caused the LC molecules to align perpendicular to the direction of the shear. The re-alignment of the LC molecules by shear stresses created a uniform diffraction of light that produced the greenish appearance of the LC (Fig. 1A).

Cell preparation

Human keratinocyte (HaCaT) cell lines were obtained from Cell Line Services (CLS, Eppelheim, Germany). Monolayers of HaCaTs were grown in Dulbecco's modified Eagle's medium (DMEM, Sigma Aldrich, Dorset, UK) supplemented with 10%

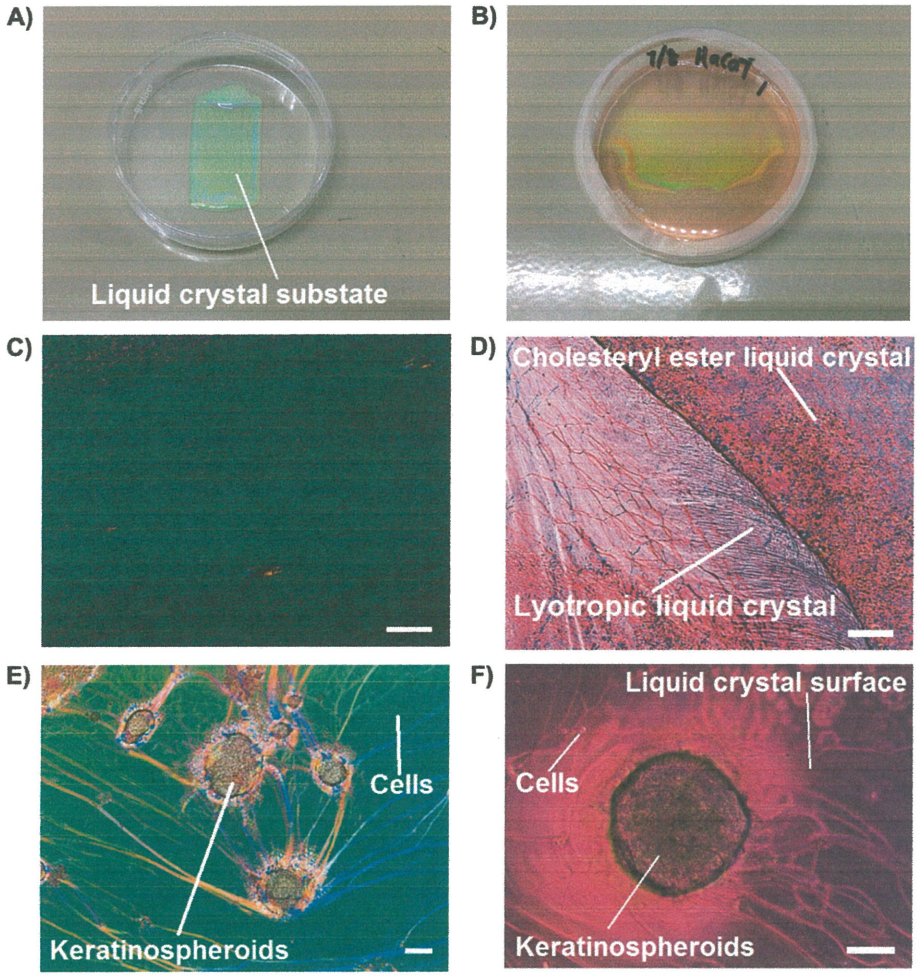

Fig. 1. A) Cholesteryl ester LC (LC) coating in a petri dish. B) 3D culture system with LC substrate. C) Crossed-polarizing microscopy of cholesteryl ester LC. D) Cholesteryl ester LC after exposure to medium. E) Crossed-polarizing microscopy of cholesteryl ester LC with the keratinospheroids. F) Phase contrast inverted microscopy of keratinospheroids on LC substrate. Scale bar = 100 μm.

fetal calf serum (PromoCell, Heidelberg, Germany), 2 mM L-glutamine (Sigma Aldrich), 2.5 mg/l fungizone (Sigma Aldrich), 100 units/ml penicillin (Sigma Aldrich) and 100 mg/ml streptomycin (Sigma Aldrich) in five 25 cm^2 tissue culture flasks. The cells were maintained in five 25 cm^2 tissue culture flasks at 37° C in a 5% CO_2 incubator. When the cells reached approximately 80% confluence, cell pellets were harvested using standard subculture procedures (Soon et al. 2014a) and placed in five 15 ml tubes before re-suspension in 5, 4, 3, 2 and 1 ml of DMEM medium. DMEM was added to the five tubes to yield cell densities of approximately 20, 40, 80, 160 and 320×10^4 cells/ml that were quantified using a hemocytometer. One milliliter from each dilution of cells was diluted further by adding 5 ml DMEM to yield cell densities of 3, 6, 12, 24 and 48×10^4 cells/ml. These cells then were ready for the 3D cell culture experiments.

3D cell culture

Six milliliters of HaCaT cells in suspension at a density of 3×10^4 cells/ml were deposited onto the surface of the LC substrate in a petri dish (Fig. 1B). As a control, cells were cultured at similar density in plain petri dishes without a LC coating. The petri dishes were sealed using paraffin film to avoid evaporation of medium. Both cell cultures were incubated at 37° C without changing medium and the cultures were monitored every 5 h using a Nikon T-100 phase contrast microscope (Nikon, Tokyo, Japan). The micrographs of the cell aggregations were captured using a Qo-5 digital camera mounted on the microscope and linked to Qcapture (version 1.0, QImaging, Surrey, Canada) software. The diameters of the keratinospheroids in the micrographs were measured using ImageJ software (National Institutes of Health, Washington, DC). The experiments were repeated three times for cell densities of 6, 12, 24 and 48×10^4 cells/ml. The cells were counted before seeding using a hemocytometer. The formation of microtissues of keratinocytes was monitored and recorded using phase contrast microscopy every 24 h for 30 days without changing the medium. Using the micrographs of microtissues, the diameters and volumes (v) of the microtissues (n = 20) were determined using the formula, $v = \frac{4}{3}\pi\left(\sqrt{r_1^2 r_2^2}\right)$, where r_1 and r_2 are the diameters of a spheroid measured in orthogonal vectors. The diameters of the keratinospheroids were measured only for spheroid microtissues. Diameters, quantities and volumes of the keratinospheroids were expressed as means ± SD.

Crossed-polarizing microscopy

We studied the optical characteristics of the LC phase using an Olympus BX53 optical microscope (Olympus, Tokyo, Japan) with a crossed-polarizers attachment at room temperature, 25° C. The cross-polarized images of the LC with and without microtissues were captured using a DP72 charge-couple-device (CCD) camera (Olympus) equipped with CellSense software (Version 1.6: Olympus).

Cell viability

For the trypan blue exclusion assay, keratinospheroids or microtissue of HaCaTs were harvested at day 5 of culture (dormant phase) and washed three times with HBSS. Five hundred microliters 0.25% EDTA-trypsin (Sigma Aldrich) was warmed on a hot plate at approximately 37° C. The keratinospheroids were transferred to the warmed EDTA-trypsin and dissociated mechanically for 10 min. Five hundred microliters DMEM was added to the cells to stop trypsinization. Subsequently, 100 µl 0.4% trypan blue (T8145; Sigma-Aldrich) was added to the cells followed by incubation at room temperature for 5 min. All viable and dead cells were counted using a phase contrast microscope. Cell viability was calculated as stained cells/(stained + unstained cells) × 100.

A live/dead cell viability kit (Invitrogen, Waltham, MA) was used to stain live and dead cells in the microtissues. Tweezers were used to place the microtissues into the depression of a concave glass slide. A solution of 0.5 µM Calcein-Am and 0.5 µM ethidium homodimer-1 in HBSS was mixed thoroughly, then added to the concave glass slide containing the microtissues for 20 min at room temperature (25° C). The fluorescent staining was observed using an Olympus BX53 fluorescence microscope (Olympus) and images were captured using a DP72 CCD camera (Olympus) linked to CellSense software (Version 1.6; Olympus). This experiment was repeated for keratinospheroids cultured on the LC substrates for 5, 10, 15 and 20 days. The live/dead cell viability kit distinguishes live from dead cells by dual staining with green-fluorescent Calcein-AM, which demonstrates intracellular esterase activity and red-fluorescent ethidium homodimer-1, which indicates loss of plasma membrane integrity.

Morphological analysis of microtissue

Microtissues of keratinocytes were removed from the surface of the LC using a Nikon stereomicroscope

and a pair of tweezers. The microtissues were washed three times in Hanks' balanced salt solution (HBSS) (Sigma Aldrich). The microtissues then were fixed with 1% formaldehyde for 10 min. Samples were washed and dehydrated through 10, 50, 75 and 95% ethanol for 5 min in each. After drying, microtissues on glass substrates were sputter-coated with gold palladium particles using an auto-fine coater (JFC-1600; JEOL, Tokyo, Japan) at 20 mA for 40 sec. The specimens were mounted on aluminium stubs with double-sided adhesive copper tape and examined using a field emission scanning electron microscope (JSM-7500F; JEOL).

Immunofluorescence staining of actin and vinculin

We used immunofluorescence staining of actin and vinculin to study the distribution of the cytoskeleton in cells of the 3D microtissue. Initially, the microtissues on a coverslip were washed five times with HBSS prior to fixation in 4% formaldehyde for 2 h. After fixation, the microtissues were washed with HBSS and permeabilized with 0.1% Triton ×-100 (Sigma Aldrich) for 5 min. For F-actin staining, the microtissues were incubated in 1 μg/ml fluorescein isothiocyanate (FITC) labeled phalloidin solution (Sigma Aldrich) in HBSS for 30 min at room temperature. The staining solution then was removed and the microtissues were washed five times with HBSS. The stained microtissue samples were incubated in 0.1 μg/ml 4',6-diamidino-2-phenylindole (DAPI) dihydrochloride (Sigma Aldrich) in HBSS for 15 min, washed and mounted on a glass slide with a spacer between the glass slide and coverslip. Monolayers of cells on the glass coverslips were cultured as controls.

Similar steps were repeated for vinculin staining, but using mouse monoclonal anti-vinculin FITC clone hVIN-1 (Sigma Aldrich) diluted 1:100 in 1% HBSS instead of FITC-labelled phalloidin. Microtissues were blocked with 2% bovine serum albumin (BSA; Sigma Aldrich) for 30 min before the samples were stained in anti-vinculin FITC for 1 h. After staining with DAPI, samples stained for actin and vinculin were observed using an Olympus BX53 fluorescence microscope (Olympus) with Plan Fluor Epi objectives (NA = 0.5) at 20 × and a DP72 CCD camera (Olympus) linked to the CellSense (Version 1; Olympus,) software mounted on the microscope.

Hematoxylin and eosin (H & E) staining

Approximately 20 200 − 300 μm pieces of microtissue were removed from the surface of the LC using forceps. The microtissues were washed, then fixed overnight in 4% formaldehyde in a 2 ml tube. After fixation for 24 h, the microtissues were centrifuged at 269 × g for 1 min. The formaldehyde was discarded and the microtissues were incubated in 70% ethanol for 3 h. Using a stereomicroscope, the microtissues were removed from the ethanol and placed in a cryomold™ (Tissue-Tek; Sakura, Sysmex Suisse AG, Horgen, Switzerland) containing frozen section compound (FSC) (Leicamicrosystem, Teban Gardens Crescent, Singapore). The cryomold™ with the microtissues embedded in FSC then was frozen at –80° C in a freezer for 15 min. The frozen block was removed from the cryomold™ and placed on a chuck with pre-deposited FSC. The chuck was allowed to equilibrate and kept frozen in a cryostat chamber (Leica CM 1850; Leica microsystem, Teban Gardens Crescent, Singapore) at –20° C for approximately 10 min. Samples were sectioned at 5 μm in the cryostat and the sections were collected on glass slides.

For H & E staining, sections of microtissues were immersed in 70% ethanol for 40 sec, then washed in distilled water. The sections were transferred to Mayer's hematoxylin to stain for 1 min. After staining, the sections were rinsed in distilled water before staining with eosin for 30 sec. After staining, the samples were dehydrated in 70, 95 and 100% alcohol. The samples were immersed in xylene for 2 min, then mounted in DPX mounting medium (Sigma Aldrich, Dorset, UK). The H & E stained samples were observed using a Nikon Eclipse E400 optical microscope (Nikon, Tokyo, Japan) (NA = 0.45, 10 x) linked to a digital camera and Qcapture (version 1.0; QImaging, Surrey, Canada) software.

Fourier transform infrared spectroscopy (FTIR) of microtissues

Three pieces of microtissue were removed from three LC 3D cultures using a bright field Nikon TS-100 inverted microscope. The tissues were washed in HBSS three times to remove residual LC gel. The monolayers of cells and microtissues were allowed to air dry for 5 min before measurements were taken. Subsequently, the samples were placed on an attenuated total reflectance (ATR) crystal window attached to a Perkin Elmer Spectrum 100 Fourier transform infrared spectrometer (Perkin Elmer, Waltham, MA). The FTIR spectrum of the microtissues and cell monolayers was recorded from 32 scans from 4000 to 600 cm^{-1} at 4 cm^{-1} resolution. Measurements for three samples were repeated three times within 2 min.

Statistical analysis

All experiments were repeated three times. The size and number of keratinospheroids were expressed as means ± SD. For comparison of the means, the data were tested for normality using the Kalmogorov Smirnov test and statistical analysis was performed using one-way analysis of variance (ANOVA) followed by Tukey HSD multiple comparisons post-test using the Statistical Package for Social Sciences (IBM-SPSS version 20) software. One-way analysis of variance was calculated to evaluate the null hypothesis that assumed no significant differences in the size of microtissues during different culture periods (n = 3) for different densities of cells. Post hoc comparisons to evaluate differences among the groups means were conducted using the Tukey HSD test, because equal variances were tenable. Values for $p \leq 0.05$ were considered significant.

Results

The cholesteryl ester LC spread in the petri dish exhibited homogeneous green reflection, which characterizes the uniform alignment of the LC molecules (Fig. 1C). With the addition of the culture medium, the LC molecules in the cholesteric phase re-oriented into the lyotropic lamellar phase and a few oil streaks could be observed in the surface of the LC (Fig. 1D) (Boltenhagen et al. 1991). The surface of LC substrate with lyotropic lamellar mesophase appeared to be a favorable platform for HaCaTs to self-assemble into keratinospheroids (Fig. 1E, F). By contrast, HaCaTs cultured on LC-free coverslips were flattened and spread out. The LC based 3D cell culture differs from the pendant drop technique, which relies on the meniscus of liquid to constrain cells in close contact (Lee et al. 2010). In LC based 3D cell culture, the cell suspension was seeded randomly onto the LC surface. The cells were attached to the LC surface after culture for 5 h; individual cells were observed migrating and merging with the cell aggregates after culture for 2 days (Fig. 2A). The number of cells in the vicinity of the aggregates increased as the culture period progressed. The assembly and aggregation of cells resulted in microspheroids with high cell density (Fig. 2A). Formation of mature microtissues, whose color approached black, was observed consistently after five days of culture (Fig. 2A). The spheroids also merged to form spheroids of greater density (Fig. 2B), which was indicated by greater absorption of light.

Without changing the medium, the microspheroids usually grew to maximum size after culture for 1 week (Fig. 3A); no expansion of spheroids was observed thereafter, which suggests that the aggregates had entered the dormant phase (Folkman and Hochberg 1973). After reaching the dormant phase at approximately 30 days of culture, the microspheroids gradually shrank and underwent necrosis (Folkman and Hochberg 1973). For keratinospheroids grown on LC substrates and without replenished nutrients, the dormant phase occurred earlier and with smaller aggregate diameters than cancerous spheroids that were grown on agar gel, which reached the dormant phase (1 mm diameter) after culture for approximately 40 days (Folkman and Hochberg 1973).

The live/dead cells viability assay demonstrated that most cells survived in the microtissues; very few dead cells were evident up to 20 days of culture (Fig. 3B); however, more dead cells were found after 20 days of culture. The results of the live/dead cell assay were confirmed by the trypan blue exclusion assay (Table 1). The average viability of microtissues of similar size (99–132 μm) after culture for 5 days on the LC substrate was approximately 80% (Table 1). The microtissues contained approximately 495–1023 cells. The size of the microtissue was inversely proportional to the viability of cells. Larger microtissues yielded greater cell densities, but a lower percentage of viable cells. This finding may be explained by the diffusion limit of thicker microtissues in multilayer of cells in which exchange of nutrients and catabolic products are restricted; this leads to starvation and death of cells at the center of the microtissue. Microtissues approximately 100 μm in diameter could increase catabolism, nutrient transport and gas exchange, which would result in a lower cell death rate (Ferro et al. 2014).

Without changing the medium, the live/dead cells viability assay indicated that majority of the cells could survive in the microtissues with very few dead cells that were stained in red up to 20 days of culture. More dead cells were found after 20 days of culture, however, as indicated by the live/dead cell staining (Fig. 3B) and further confirmed by the trypan blue exclusion assay (Table 1).

We investigated the optimal cell densities that would enable the formation of keratinospheroids using five cell densities to determine the number and size of spheroids generated (Fig. 4A). We found significant differences between the mean size of microspheroids cultured for 24 and 48 h ($p = 0.036$, n = 3), 24 and 72 h ($p = 0.025$, n = 3), and 48 and 72 h ($p = 0.045$, n = 3) at 6×10^4 cells/ml. At 12×10^4 cells/ml, we observed significant differences only between 24 and 48 h ($p = 0.005$, n = 3), 24 and 72 h ($p = 0.001$, n = 3), and 48 and 72 h ($p = 0.002$, n = 3).

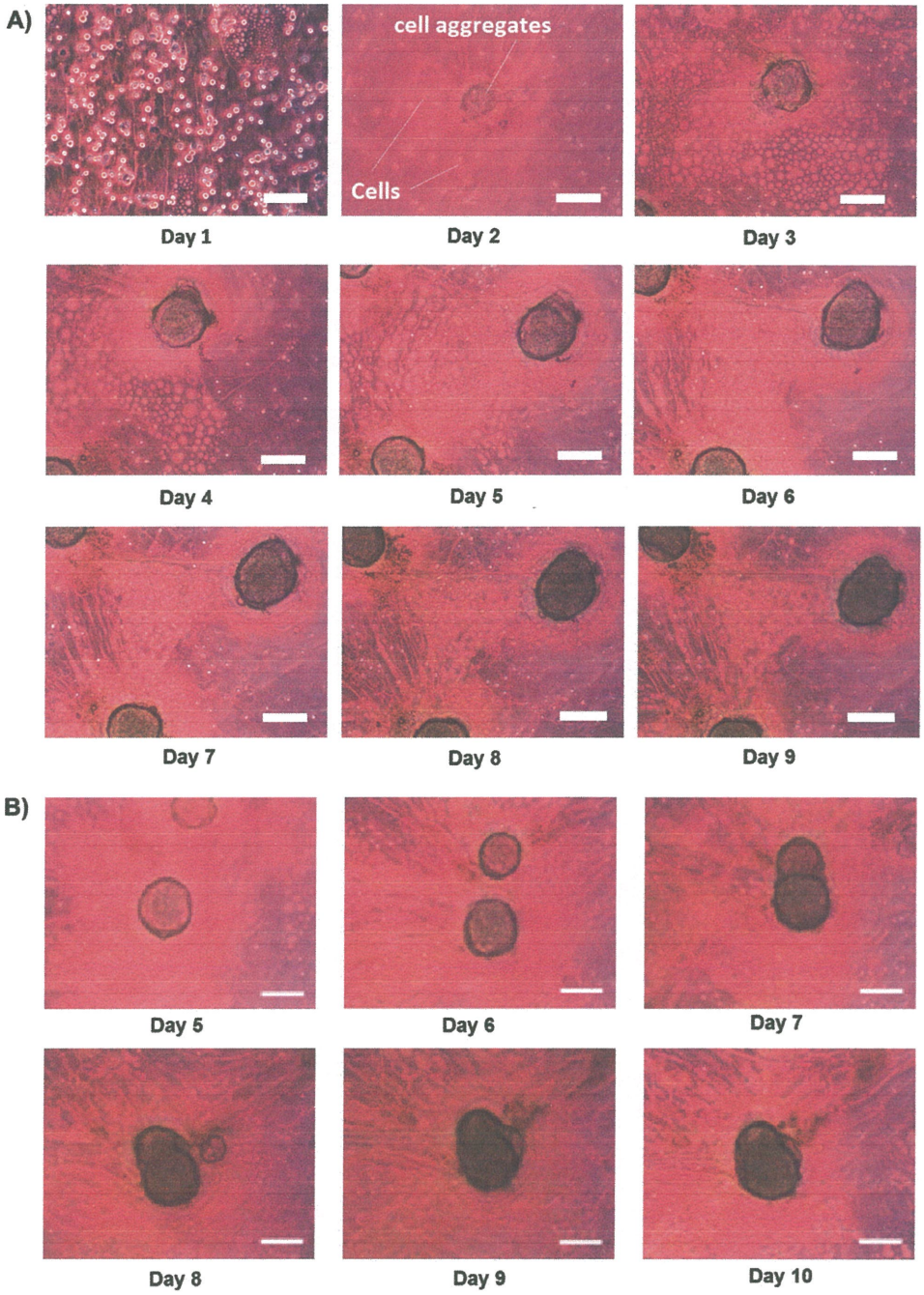

Fig. 2. A) Formation of 3D microspheroids from initial formation to maturation. Day 7 onward is the optimal culture period for obtaining matured keratinospheroids. B) Migration and integration of keratinospheroids. Scale bar = 100 μm.

At 24×10^4 cells/ml, we found significant differences between 24 and 48 h ($p = 0.001$, n = 3), 24 and 72 h ($p = 0.001$, n = 3), but no statistically significant differences ($p = 0.135$, n = 3) for 48 and 72 h.

We found no significant differences in the size of the keratinospheroids when cells were plated at densities of 3×10^4 and 48×10^4 cells/ml. The size of the microspheroids stabilized after culture for 72 h at approximately 158 ± 47 μm at a cell density of 24×10^4 cells/ml (Fig. 4A). The growth of microspheroids depends more on culture periods than on cell densities.

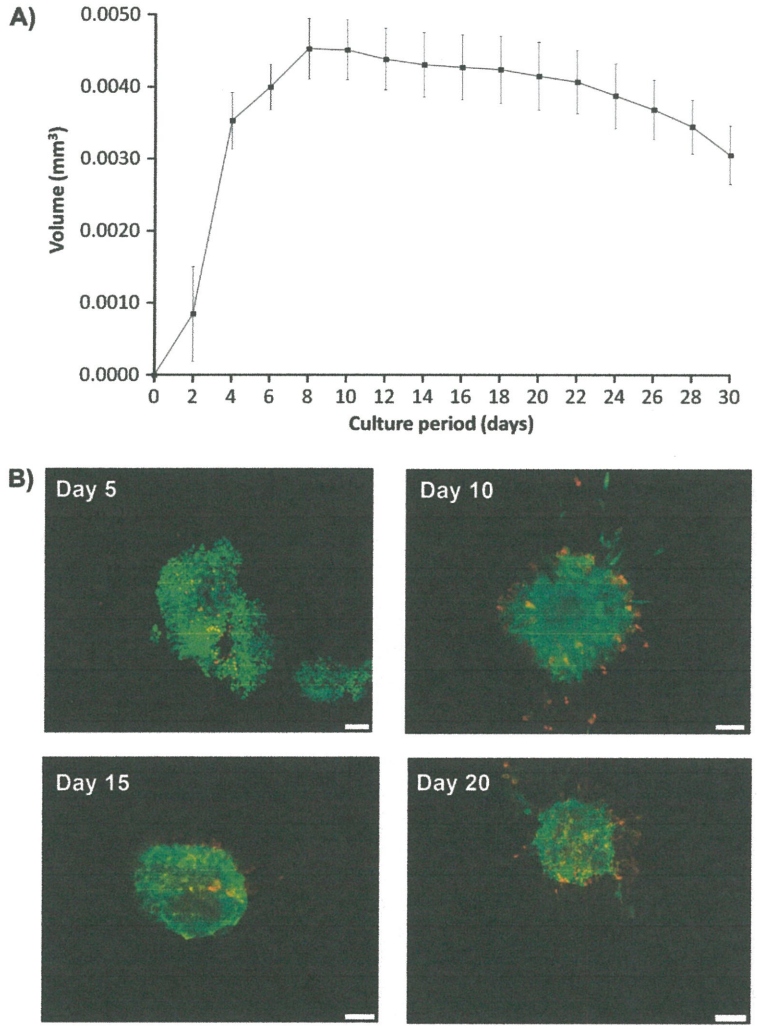

Fig. 3. A) Growth, dormant and necrosis phases of HaCaTs microspheroids. Microtissues after day 7 began to shrink, which indicated the necrosis phase of the 3D cells. Error bars indicate standard deviation of the volume of spheroids. B) Live and dead cells in microtissues at 5, 10, 15 and 20 days of culture on LC substrate. Cells labeled green and red using Calcein-Am and ethidium homodimer-1 indicate live and dead cells, respectively. Scale bar = 100 μm.

The number of spheroids increased proportionally (20–50/petri dish) as the cell density (3–24 $\times 10^4$ cells/ml) increased. Differences in the numbers of keratinospheroids, however, did not differ for cell densities ranging from 3–12 $\times 10^4$ cells/ml. When the cell density reached 24 $\times 10^4$ cells/ml, the number of keratinospheroids showed statistically significant differences among the three culture periods ($p = 0.001$, n = 3). During 3 days of observation, the number of spheroids was consistently low when the cell culture density increased beyond 48 $\times 10^4$ cells/ml. At 48 $\times 10^4$ cells/ml, the number of

Table 1. Physical characteristics and cell viability of keratinospheroids

Keratinospheroid	Radius (μm)	Volume (mm^3)	Viable cells	Dead cells	Cell viability (%)
1	99.49	0.0041	495	98	83.47
2	110.14	0.0056	667	140	82.65
3	132.47	0.0097	1023	260	80.73

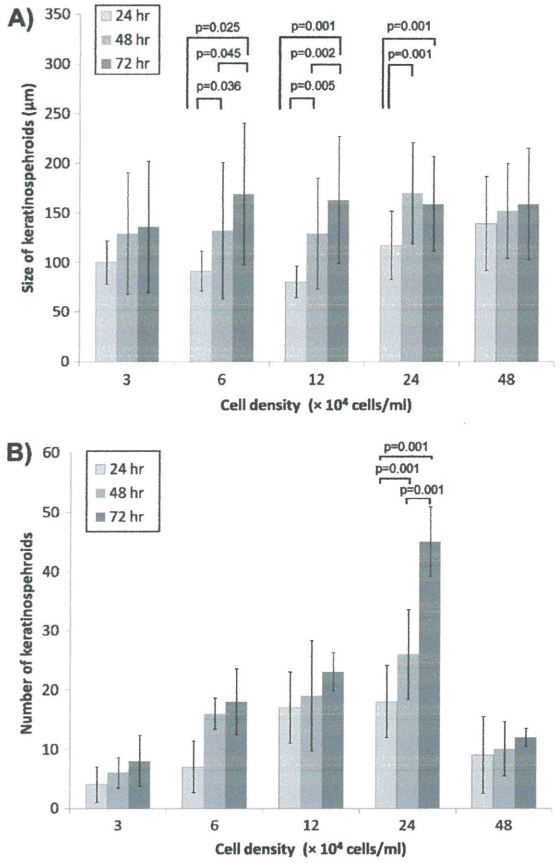

Fig. 4. A) Diameters of spheroids (means ± SD) at varying cell densities after culture for 24, 48 and 72 h (n = 3). B) Number of spheroids formed. The data are significantly different for groups cultured at 24 × 10^4 cells/ml.

spheroids decreased significantly compared to 24×10^4 cells/ml as shown in Fig. 4B. The number of keratinospheroids was reduced, because microspheroids merged into large masses of microtissues when the cell density was $\geq 48 \times 10^4$ cells/ml.

Using FE-SEM, we found that the morphology of the microtissues cultured on the LC surface was homogenous (Fig. 5A–C). The surface structure of the microspheroids suggested that cells regained intercellular integrity and good intercellular adhesion by self-assembly of cells on the LC substrate (Fig. 5B). The microspheroids harvested from the culture had a diameter of 500 µm and thickness of approximately 100 µm (Fig. 5C). The thin layer of multi-stratified cells may permit sufficient internalization of nutrients and oxygen from the medium by the innermost cells; this appears to occur readily when the thickness of microtissues is < 300 µm (Yamada and Cukierman 2007).

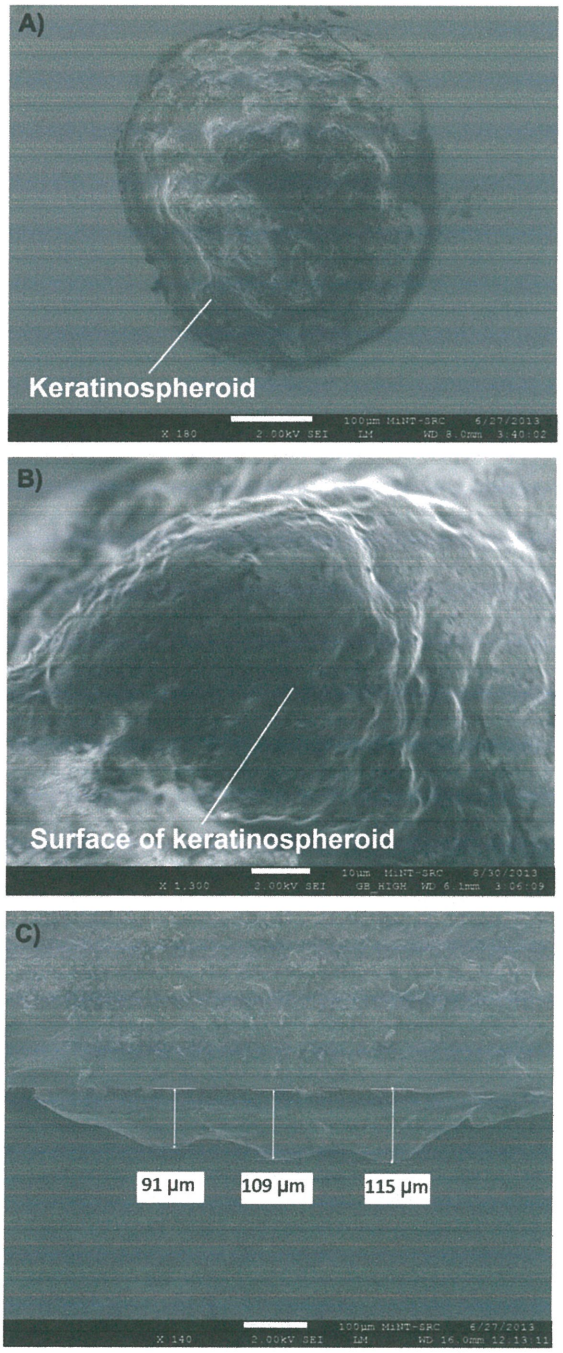

Fig. 5. Field-emission scanning electron of keratinospheroids. A) Top view of the keratinospheroid. Scale bar = 100 µm. B) Surface morphology of the keratinospheroid. Scale bar = 10 µm. C) Thickness of microspheroid. Scale bar = 100 µm.

We observed expression of punctuated vinculins coupled to diffuse actin filaments by the keratinospheroids on the LC substrate (Fig. 6A, B).

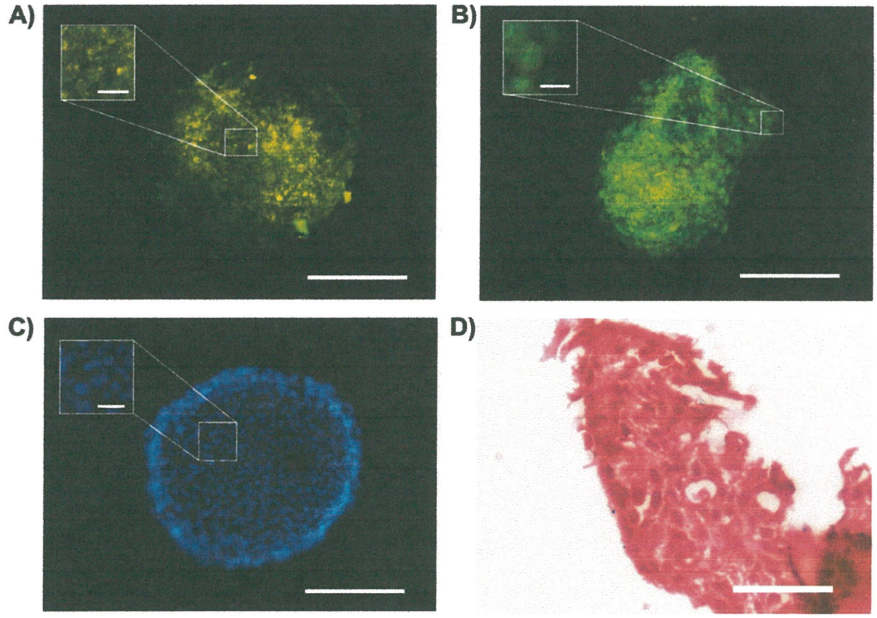

Fig. 6. Immunofluorescence staining of keratinospheroids. A) Vinculin (green). B) Actin (green). C) Nuclei (blue). D) H & E staining of section of keratinospheroids showing nuclei (purple) and cytoplasm (pink). Insets are 5 ×. Scale bars = 100 μm, inset scale bar = 10 μm.

Expressions of both cytoskeletal elements were distinctly different from those observed in monolayers of HaCaT cells grown on hard substrates (Soon et al. 2014a). Cells in 2D cultures are characterized by striated stress fibers and distribution of classical angular vinculin accumulations (Discher et al. 2005). Staining of the cell nuclei (Fig. 6C) and vinculins (Fig. 6A) in microspheroids revealed that cells were organized compactly.

Consistent with our FE-SEM results, the thickness of the microtissues in the histological sections (Fig. 6D) was approximately 100 μm, which is close to the thickness of the human skin epidermis (Hendriks et al. 2006, Takeo 2007). Multilayers of cells with rounded nuclei were organized into stratified layers in the microtissues and cells at the margins of the keratinospheroids assumed a flattened morphology, which bore some similarity to the stratified squamous epithelial layer of skin (Fig. 6D).

Figure 7 shows the FTIR spectrum from 600 to 4000 cm^{-1} of a keratinospheroid. The main infrared absorption bands at 1641, 2926 and 3283 cm^{-1} are due to lipid CH_3, lipid CH_2, and protein, respectively. The absorption above 3000 cm^{-1} indicated O-H stretching that was attributed to traces of water; in the repeated experiments, the absorption band above 3000 cm^{-1} depended on the state of hydration of the samples. Intense amide I and

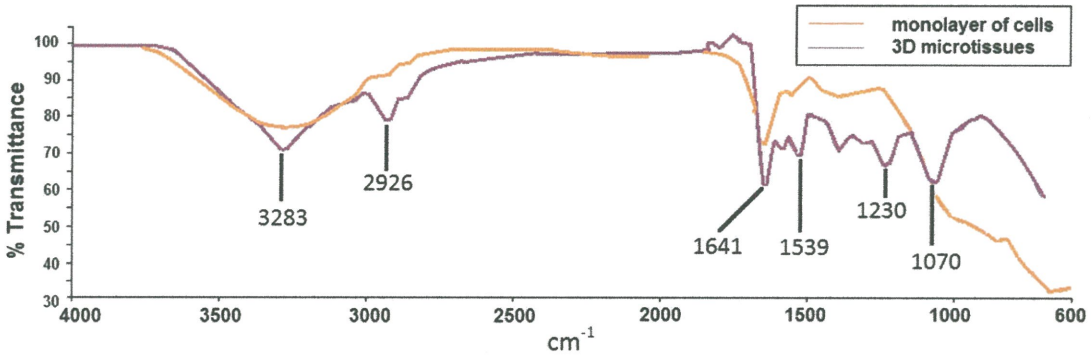

Fig. 7. Transmittance of FTIR spectrum for monolayer of cells and 3D microtissues.

II absorptions at 1539 and 1641 cm^{-1} were due to C-N-H bending vibrations and C = O stretching, respectively. Consequently, the absorptions of the two amide groups indicated the protein absorptions of the microtissues (Jackson and Mantsch 1995). The ionized asymmetric stretching of PO^{-2} exhibited strong absorptions at 1070 and 1230 cm^{-1} that could be attributed to the presence of nucleic acid in the microtissues. To examine the difference in the absorption of the microtissue and the monolayer of cells, we calculated the intensity ratio of the amide I:II associated with the carbonyl group of deoxyribonucleic acid (DNA) (Prabhakar et al. 2012, Ramesh et al. 2002, Ramesh et al. 2001). The intensity ratios of absorptions at 1539 and 1641 cm^{-1} for the microtissue and the monolayer of cells were 1.167 and 1.133, respectively. The ratios indicate increased DNA absorption by the keratinocytes in the microtissues compared to the monolayer of cells that could be attributed to the difference in the structure of the cells organization (Fig. 7). Overall, cell monolayers exhibited less intense absorptions for nucleic acid, amide and lipid groups at 1070, 1230, 1539, 1641 and 2926 cm^{-1}.

Discussion

Our method requires simple squeegee coating of LC gel onto the surface of petri dishes. The LC surface induces randomly distributed keratinocytes in the culture to self-assemble and self-stratify into 3D structures without scaffolds as required by other methods (Amann et al. 2014, Svoronos et al. 2014). The 3D cell model presented here might be used to study blocking of signaling pathways associated with self-organization, migration and differentiation of cells; which in turn would provide information about whether the cells can form keratinospheroids after disruption of signaling pathways.

The ability of cells to self-organize into 3D microstructures may be due to the physical properties of the LC. The soft compliance of the LC at approximately 100 kPa is similar to the stiffness of the epidermis (Hendriks et al. 2006, Soon et al. 2013b, Takeo 2007); therefore, it provides a mechanical environment that encourages the formation of cells into 3D structures. Soluble biomolecules in the culture medium also can influence the formation of microspheroids. Classic keratinocyte stratification medium has been used to stimulate the proliferation of epidermal cells on collagen gels for stratification of keratinocytes in a 3D organotypic culture (Ma et al. 2009). In organotypic models, morphogenesis of epidermis requires supplements of cytokines and growth factors (Ma et al. 2009). Therefore, we used DMEM medium supplemented with FBS, penicillin, streptomycin, fungizone, L-glutamine and soluble growth factors.

We monitored our 3D cultures for 30 days without changing the medium, which enabled our investigation of the fundamental growth of 3D keratinospheroids to the dormant phase. The arrest of cell growth during the dormant phase at the plateau phase (Fig. 3) indicates self-regulation. The plateau phase is the region in the curve (Fig. 3) where the size of the keratinospheroids is characterized by similar volumetric changes. The whole time course of volumetric changes of the keratinospheroids in a sigmoidal pattern as shown in Fig. 3 is closely related to a typical growth curve for normal cultured cells.

The homogeneous surface of the microtissue in the FE-SEM images indicated good intercellular adhesion (Amann et al. 2014), which suggested that the tight attachments of cells on the surface of microspheroids could be associated with enhanced ECM production and enhanced intercellular attachment. Histological sections revealed that the cells were polarized parallel to the elongated axis of the spheroid (Fig. 6D) and that cells at the periphery acquired a more flattened morphology. FTIR indicated that the 3D keratinospheroids cultured on the LC surface contained more lipid and nucleic acids than keratinocytes grown in a 2D culture environment. Therefore, our FTIR results indicate that the stratification of cells of 3D keratinospheroids exerts a greater effect on the up-regulation of biological compounds compared to 2D monolayer cells. In cell monolayers, some functional groups were down-regulated, which may be due to loss of intercellular and ECM related communication pathways.

Monitoring the contraction response and biophysical changes of 3D cell models to different doses of TGF-β may provide more insight into the role of cytokines in wound repair (Decline et al. 2003, Garlick and Taichman 1994). Future study should focus on the effects of TGF-β1 on biophysical changes using the 3D cell model described here; the 3D model of keratinospheroids would provide tissue in vitro that is closer to epithelium. Three-dimensional cell culture based on LC also can be used to study the effects of knockout of specific signaling pathways that regulate the migration ability of epithelial cancer cells, which might impede the growth of cancer cells.

We have described the use of LC as a substrate for culturing randomly distributed keratinocytes into 3D microtissues without scaffolds. Keratinocytes migrated and self-organized into 3D

keratinospheroid-like structures on the LC surface. Without changing the medium, keratinospheroids reached dormancy after five days in culture and continued to survive at approximately 80% viability for up to 20 days of culture. Cell density did not influence the size of the keratinospheroids formed, but it did affect the number of spheroids formed. Using our technique, good adhesion of cells in stratified keratinospheroids was attained. The self-assembly of cells to form keratinospheroids produced a diffuse cytoskeleton and small punctuate vinculins. FTIR spectroscopy detected greater expression of lipid and nucleic acid in 3D microtissues compared to 2D cultured cells. Our technique enables observation of both cell and keratinospheroid migrations that may be useful for studying the mobility of cancer microtissues and characterizing the cell signalling that other 3D cell culture techniques may not permit (Amann et al. 2014, Svoronos et al. 2014, Tibbitt and Anseth 2009).

Acknowledgments

We thank Professor Dr. Gan Siew Hua from Universiti Sains Malaysia for her help with proofreading this manuscript. The authors are grateful to the research financial support (Science Fund Vot No.: 0201-01-13-SF0104 or S024) awarded by Malaysia Ministry of Science and Technology (MOSTI).

Declaration of interest: The authors report no conflicts of interest. The authors alone are responsible for the content and writing of this paper.

References

Amann A, Zwierzina M, Gamerith G, Bitsche M, Huber JM, Vogel GF, Blumer M, Koeck S, Pechriggl EJ, Kelm JM, Hilbe W, Zwierzina H (2014) Development of an innovative 3D cell culture cystem to study tumour-stroma interactions in non-small cell lung cancer cells. *PLoS One* 9: 92511–92513.

Boltenhagen P, Lavrentovich O, Kleman M (1991) Oily streaks and focal conic domains in lyotropic liquid crystals. *J. Phys. II* 1: 1233–1252.

Bruce DW, Goodby JW, Sambles JR, Coles HJ (2006) Introduction: new directions in liquid crystal science. *Phil. Trans. Roy. Soc. A* 364: 2567–2571.

Decline F, Okamoto O, Mallein-Gerin F, Helbert B, Beranud J, Rigal D, Rousselle P (2003) Keratinocyte motility induced by TGF-beta1 is accompanied by dramatic changes in cellular interactions with laminin 5. *Cell Motil. Cytoskel.* 54: 64–80.

Discher DE, Janmey P, Wang Y-l (2005) Tissue cells feel and respond to the stiffness of their substrate. *Science* 310: 1139–1143.

Feingold K (2007) The role of epidermal lipids in cutaneous permeability barrier homeostasis. *J. Lipid Res.* 48: 2531–2546.

Ferro F, Baheney CS, Spelat R (2014) Three-dimensional (3D) cell culture conditions, present and future improvements. *Raz. Int. J. Med.* 2: 17801–17809.

Folkman J, Hochberg M (1973) Self-regulation of growth in three dimesions. *J. Exp. Med.* 138: 745–753.

Garlick JA, Taichman LB (1994) Effect of TGF-β1 on re-epithelialization of human keratinocytes in vitro: an organotypic model. *J. Invest. Dermatol* 103: 554–559.

Grabowska I, Szeliga A, Moraczewski J, Czaplicka I, Brzóska E (2011) Comparison of satellite cell-derived myoblasts and C2C12 differentiation in two- and three-dimensional cultures: changes in adhesion protein expression. *Cell Biol. Int.* 35: 125–133.

Harma V, Virtanen J, Makela R, Happonen A, Mpindi J-P, Knuuttila M, Kohenen P, Lotjonen J, Kallioniemi O, Nees M (2010) A comprehensive panel of three-dimensional models for studies of prostate cancer growth, invasion and drug responses. *PLoS One* 5: 10431–10417.

Hata Y, Shigematsu H, Insull W (1980) Cholesteryl ester-rich inclusions from human aortic fatty streak and fibrous plaque lesions of atherosclerosis. II. Physical properties of swelling, resiliency and lyotropy as liquid crystal. *Jpn. Circ. J.* 44: 46–54.

Hendriks FM, Brokken D, Oomens CWJ, Bader DL, Baaijens FPT (2006) The relative contributions of different skin layers to the machanical behavior of human skin in vivo using suction experiment. *Med. Eng. Phys.* 28: 259–266.

Hsieh C-H, Wang J-L, Huang Y-Y (2011) Large-scale cultivation of transplantable dermal papilla cellular aggregates using microfabricated PDMS arrays. *Acta Biomater.* 7: 315–324.

Huh D, Hamilton Geraldine A, Ingber DE (2011) From 3D cell culture to organs-on-chips. *Trends Cell Biol.* 21: 745–754.

Hwang JJ, Iyer SN, Li L-S, Claussen R, Harrington DA, Stupp IS (2002) Self-assembling biomaterials: liquid crystal phases of cholesteryl oligo(l-lactic acid) and their interactions with cells. *Proc. Natl. Acad. Sci. USA* 99: 9662–9667.

Ingber DE (2006) Cellular mechanotransduction: putting all the pieces together again. *FASEB J.* 20: 811–827.

Jackson M, Mantsch HH (1995) The use and misuse of FTIR spectroscopy in the determination of protein structure. *Crit. Rev. Biochem. Mol. Biol.* 30: 95–120.

Kravchenko I, Boyko Y, Novikova N, Egorova A, Andronati S (2011) Influence of cholesterol and its esters on skin penetration in vivo and in vitro in rats and mice. *Ukr. Bioorg. Acta* 17-21.

Kunz-Schughart LA, Freyer JP, Hofstaedter F, Ebner R (2004) The use of 3-D cultures for high-throughput screening: the multicellular spheroid model. *J. Biomol. Screen.* 9: 273–285.

Lee JM, Mhawech-Fauceglia P, Lee N, Parsanian LC, Lin YG, Gayther SA, Lawrenson K (2013) A three-dimensional microenvironment alters protein expression

and chemosensitivity of epithelial ovarian cancer cells in vitro. *Lab. Invest.* 93: 528–542.

Lee WG, Ortmann D, Hancock MJ, Bae H, Khademhosseini A (2010) A hollow sphere soft lithography approach for long-term hanging drop methods. *Tissue Eng. Part C* 16: 249–259.

Loessner D, Stok KS, Lutolf MP, Hutmacher DW, Clements JA, Rizzi SC (2010) Bioengineered 3D platform to explore cell-ECM interactions and drug resistance of epitherlial ovarian cancer cells. *Biomaterials* 31: 8494–8506.

Ma K, Laco F, Ramakrishna S, Liao S, Chan CK (2009) Differentiation of bone marrow-derived mesenchymal stem cells into multi-layered epidermis-like cells in 3D organotypic co-culture. *Biomaterials* 30: 3251–3258.

Napolitano AP, Dean DM, Man AJ, Youssef J, Ho DH, Rago AP, Lech MP, Morgan JR (2007) Scaffold-free three-dimensional cell culture utilizing micromolded nonadhesive hydrogels. *BioTechniques* 43: 494–500.

Norlen L, Plasencia Gil I, Simonsen A, Descouts P (2007) Human stratum corneum lipid organization as observed by atomic force microscopy on Langmuir-Blodgett films. *J. Struct. Biol.* 158: 386–400.

Peyton SR, Kim PD, Ghajar CM, Seliktar D, Putnam AJ (2008) The effects of matrix stiffness and RhoA on the phenotypic plasticity of smooth muscle cells in a 3-D biosynthetic hydrogel system. *Biomaterials* 29: 2597–2607.

Prabhakar S, Jain N, Singh RA (2012) Infrared spectra in monitoring biochemical parameters of human blood. *J. Phys. Conf. Ser.* 365: 012051–012055.

Ramesh J, Salman A, Mordechai S (2001) FTIR microscopic studies on normal, polyp, and malignant human colonic tissues. *Sub. Sens. Tech. Appl.* 2: 99–117.

Ramesh J, Argov S, Salman A, Yuzhelevski M, Sinelnikov I, Goldstein J, Erukhimovitch V, Mordechai S (2002) Spectroscopic evidence for site-specific cellular activity in the tubular gland in human intestine. *Eur. Biophys. J.* 30: 612–616.

Small DM (1977) Liquid crystals in living and dying systems. *J. Coll. Interface Sci.* 58: 581–602.

Soon CF, Youseffi M, Gough T, Blagden N, Denyer MCT (2011) Rheological characterization of the time-dependent cholesteric based liquid crystals and in-situ verification. *Mater. Sci. Eng. C* 31: 1389–1397.

Soon CF, Ali Khaghani S, Youseffi M, Nayan N, Saim H, Britland S, Blagden N, Denyer MCT (2013a) Interfacial study of cell adhesion to liquid crystals using widefield surface plasmon resonance microscopy. *Col. Sur. B: Bio.* 110: 156–162.

Soon CF, Youseffi M, Berends RF, Blagden N, Denyer MCT (2013b) Development of a novel liquid crystal based cell traction force transducer system. *Biosens. Bioelectron.* 39: 14–20.

Soon CF, Omar WIW, Berends RF, Nayan N, Basri H, Tee KS, Youseffi M, Blagden N, Denyer MCT (2014a) Biophysical characteristics of cells cultured on cholesteryl ester liquid crystals. *Micron* 56: 73–79.

Soon CF, Goh ZP, Ku LC, Lee TT, Tee KS (2014b) A squeegee coating apparatus for producing a liquid crystal based bio-transducer. *Appl. Mech. Mater.* 465: 759–763.

Svoronos AA, Tejavibulya N, Schell JY, Shenoy VBa, Morgan JR (2014) Micro-mold design controls the 3D morphological evolution of self-assembling multi-cellular microtissues. *Tissue Eng.* 20: 1134–1144.

Takeo M (2007) Skin biomechanics from microscopic viewpoint: mechanical properties and their measurement of horny layer, living epidermis, and dermis. *Fagr. J.* 35: 36–40.

Tibbitt MW, Anseth KS (2009) Hydrogels as extracellular matrix mimics for 3D cell culture. *Biotechnol. Bioeng.* 103: 655–663.

Unna PG, Goldsdetz L (1910) Biochemistry *25*: 425–431.

Yamada KM, Cukierman E (2007) Modeling tissue morphogenesis and cancer in 3D. *Cell* 130: 601–610.